

MODELING OF RF ABSORBER FOR APPLICATION IN THE DESIGN OF ANECHOIC CHAMBER

B.-K. Chung and H.-T. Chuah

Faculty of Engineering
Multimedia University
Persiaran Multimedia
63100 Cyberjaya, Malaysia

Abstract—A proper model of RF absorber must be developed based on information such as absorber reflectivity, in magnitude and phase, for various angles of incidence, and for parallel and perpendicular polarizations. Unfortunately, these data are not available due to the practical limitations of the test fixtures to measure the RF absorber performance. Manufacturer data sheets normally specify only the magnitude of the absorber reflectivity for normal incidence. A model has been developed in this paper for pyramidal RF absorber with pyramid length shorter than a quarter wavelength and poor reflectivity performance. Since the reflection from the metal backing would be much higher than the reflection and scattering from the pyramid tips, the metal boundary may be modeled as a lossy dielectric with certain effective dielectric constant, ϵ_{eff} , and effective conductivity, σ_{eff} , and the thickness extends to infinity. The appropriate values of ϵ_{eff} and σ_{eff} can be derived based on the reflectivity information given by the manufacturer's data sheet. The reflectivity at oblique incidence is calculated and compared with the results of method of homogenization and moment method. A reasonable match between the different models is obtained. The plane-boundary dielectric model can be used to evaluate the degradation of reflectivity level with respect to angle of incidence. It can be used in a simulation tool for design of anechoic chamber.

1 Introduction

2 Modeling of RF Absorber

3 A Plane-Boundary Lossy Dielectric Model

4 Conclusions

Acknowledgment

References

1. INTRODUCTION

Electromagnetic wave measurements involving very low signal levels are commonly performed in laboratory facilities that provide high isolation from external electromagnetic environment. Shielded enclosures with isolation performance in excess of 100 dB prevent extraneous energy from masking measurements of the intended signals. However, electromagnetic wave generally propagates in all directions and waves reflected by the walls, ceiling, and floor of the shielded enclosure will give rise to a complex wave front at the test region where the test antenna is to be placed. As it is desirable to provide an environment for electromagnetic energy to propagate between the test antenna and the device-under-test (DUT) in a simple and well defined manner, waves propagating towards the walls, ceiling, and floor of the enclosure must be absorbed using a suitable absorbing material. A shielded enclosure with the entire inner surfaces covered with wave absorber to create a non-reflecting environment equivalent to free space is known as Anechoic Chamber.

Anechoic chambers are mostly utilized in the microwave region. Much research has been focusing on developing absorbers with superior absorbing properties such as low normal-incidence reflection, low forward-scatter and backscatter at wide-angle incidence, lower usable frequency, wide bandwidth, and reduced absorber thickness [1] in the course of improving the “quietness” of anechoic chambers, cost efficiency and required room size. The idea of using material which gradually tapers from impedance near that of free space at the front surface to that of a lossy medium at the back surface has dominated this area of development. One implementation of such idea is to shape the absorbing material into wedge or pyramid shape in contrast to flat front surface. The height of the pyramid must be greater than quarter wavelength to function efficiently. At 30 MHz, the taper length must be greater than 2.5 m. The bulky size gives rise to high cost of material, installation difficulty, and requirement for large room space.

An increasing number of low-frequency (30–1000 MHz) electromagnetic anechoic and semi-anechoic test chambers have been manufactured in recent years due to the rapid growth in multimedia and telecommunication industries. Products must meet both emission and immunity requirements of electromagnetic compatibility (EMC) regulation before they can be marketed. A full anechoic chamber is com-

monly used to determine the immunity of products to impinging electromagnetic field. As for the emission limit, interference emissions from electronic products are referenced to measurements performed on an ideal Open Area Test Site (OATS) having a perfectly conducting infinite ground-plane. A semi-anechoic chamber in which the conductive floor is not covered with wave absorbing material can be used as the alternative test site for this measurement.

Ferrite tile is a new generation of low-frequency broadband absorber that has been widely used in many EMC test chamber. The ferrite tile (NiZn) with a thickness of 6-mm may offer a reflectivity level below -15 dB over the frequency range of 30 to 600 MHz but the reflectivity deteriorates rapidly as the frequency goes higher [2]. Thin urethane foam pyramids that are optimized to operate from 200 to 1000 MHz have been combined with ferrite tiles to form a hybrid absorber to cover the required frequency range of 30–1000 MHz. The ferrite tiles and hybrid absorbers are extremely expensive. In addition, the strength of the room must be strong enough to support the weight of the tiles (greater than 30 kg/m^2). The special room structure adds to the cost of constructing the anechoic chamber. On the other hand, the use of 2.5-m thick pyramid absorbers requires a screened room size larger than $20 \text{ m} \times 10 \text{ m} \times 9 \text{ m}$ height in order to construct a 10-m range semi-anechoic chamber for EMC tests. The required cost and space are substantial. Hence, there is much interest in trying to reduce the required investment while still maintaining adequate performance.

Anechoic chambers that are built specifically for EMC tests are usually not suitable for radar cross-section and antenna measurements. Similarly a microwave anechoic chamber using pyramidal foam absorbers with thickness less than 1 m is usually not suitable for EMC tests. For example, a 0.6-m (24-inch) pyramid absorber can typically give a reflectivity level lower than -20 dB only at frequencies above 200 MHz. However, if the chamber geometry is designed such that an electromagnetic ray from the transmitter will only reach the receiver antenna after a few reflections, the wave energy may be sufficiently damped after a few bounces off the absorbing walls and ceiling. Hence, the usable frequency range of a microwave anechoic chamber may be extended to cover the 30–1000 MHz frequencies for EMC tests. An appropriate model of the absorber is required for prediction of the anechoic chamber performance prior to the construction.

2. MODELING OF RF ABSORBER

The calculations of the interference field in an anechoic chamber are often inaccurate due to the lack of a proper model to characterize the

scattering behavior of absorbers when they are lined up on the chamber walls. With the transmitter located at one end of the chamber and the receiver located at the other end, the reflected waves in magnitude and phase must be known in order to calculate the total field due to the sum of the direct wave and the reflected waves. Absorber manufacturers usually specify only the reflectivity at normal incidence due to the limitation of the large waveguide or large coax line that are used to carry out the measurement [3, 4]. In actual fact, the reflectivity at oblique incidence may deteriorate rapidly with increasing incident angle. An engineering model of the absorber must be developed based on information such as absorber reflectivity, in magnitude and phase, for various angles of incidence, from normal to grazing angles, and for parallel and perpendicular polarizations.

For an array of pyramids, the equivalent permittivity and permeability have often been assumed to be the spatial averages between those of air and the absorber. The simple averages are incorrect because the absorber array actually behaves as an inhomogeneous medium. A technique called the method of homogenization has been developed by Kuester and Holloway [5] for modeling of pyramidal and wedge shaped absorbers. The gradually changing impedance from free space wave impedance at the pyramid tip to that of the lossy dielectric slab at the base is modeled as multi-layered structure consisting of thin planar layers of absorbing medium possessing certain effective permittivity and permeability (see Figure 1). A Transmission Line modeling technique is then used to calculate the reflection coefficient of the multi-layered absorbing material backed by conducting plane.

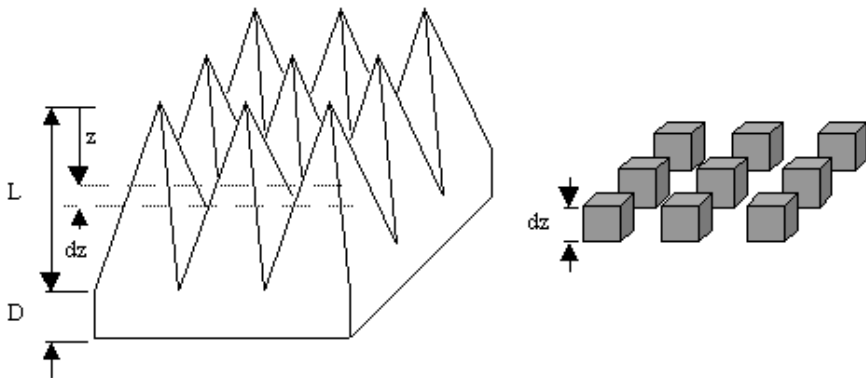


Figure 1. Array of square absorbing blocks representing a layer of the pyramid absorber.

A numerical electromagnetic computation method such as the method of moment can be used for modeling of pyramid absorber [6]. However, the material properties of the absorber are usually considered as proprietary information of the manufacturers. If samples of the absorbers are available, the bulk parameter can be obtained from *s*-parameter measurement of coaxial or waveguide fixture filled with the RF absorber material. Multiple samples extracted from several places of the absorber shall be tested. Generally, a great variation of the bulk parameters throughout the RF absorber block will be found.

The final use of absorber is not as isolated small piece of material. In the design of an anechoic chamber, the engineer has to know the performance of the RF absorber tiles in typical array configurations. The great variation of bulk parameters as well as gaps in lining the absorber material over the area illuminated by a plane wave may result in large error of the actual reflection coefficient compared to the calculated value. The mounting methods used in the absorber installation (thickness of adhesive, mounting bracket, etc.) may also contribute to additional errors. In some situations, the RF absorber is illuminated at near field by a spherical wave (with wave impedance deviates from 377 ohms) rather than a plane wave. Therefore, the assumption of plane wave illumination in the calculation will be invalid. Since the degradation of RF absorber performance with respect to angle of incidence cannot be easily verified, the use of a simplified model for RF absorber will suffice to give a reasonable prediction or estimation on the effectiveness of the RF absorber in actual applications. The use of a complex model may not give a more accurate result due to the various uncertainties involved.

3. A PLANE-BOUNDARY LOSSY DIELECTRIC MODEL

When electromagnetic wave illuminates a RF absorber with metal backing, three physical processes take place:

- reflection and scattering of the incident wave from the absorber surface,
- absorption of the refracted wave by the lossy absorber material, and
- reflection of the attenuated refracted wave from the metal backing, propagating through the absorber and air to the field sensor.

At low RF frequency when the pyramid length is shorter than a quarter wavelength, pyramidal absorber may have a poor reflectivity performance. The absorber would dissipate only a limited amount of energy of the incident wave. The reflection from the metal backing

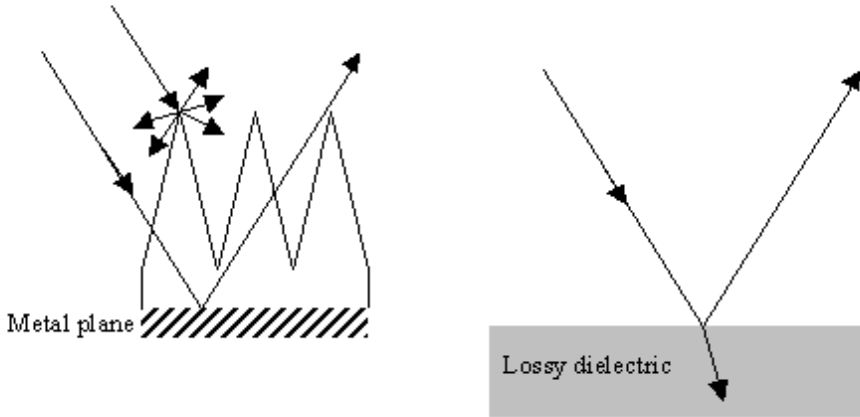


Figure 2. Plane-boundary lossy dielectric model for pyramidal absorber.

would be much higher than the reflection and scattering from the pyramid tips. Hence, the metal boundary may be modeled as a lossy dielectric with an effective dielectric constant, ε_{eff} , and an effective conductivity, σ_{eff} , as illustrated in Figure 2. Since the refracted wave into the medium is not required, the lossy dielectric model can have an infinite thickness. Assuming a relative permeability of 1, the complex permittivity of the lossy dielectric may be written as

$$\varepsilon_r = \varepsilon_{eff} - j \frac{\sigma_{eff}}{\omega \varepsilon_0} \quad (1)$$

where ω is the radian frequency and ε_0 is permittivity of free space.

The reflectivity of pyramidal absorbers generally decreases exponentially with frequency. The similar frequency response may be observed in the reflection characteristics for wave incidents on a plane-boundary lossy dielectric. The appropriate values of ε_{eff} and σ_{eff} can be derived based on the reflectivity information given by the manufacturer's data sheet.

A nonlinear least-squares optimization method has been used. First, the values of ε_{eff} and σ_{eff} are arbitrarily selected. The reflection coefficients at normal incidence for a number of frequency points are calculated using Equation (2). A sum-of-square for the deviations of these reflection coefficients $\Gamma(\varepsilon_{eff}, \sigma_{eff}, \omega_i)$ compared to manufacturer data $\Gamma_m(\omega_i)$ at various frequencies is then evaluated using Equation (3). An iteration process to minimize the sum-of-square error is carried

out to obtain the optimum values of ϵ_{eff} and σ_{eff} .

$$\Gamma(\epsilon_{eff}, \sigma_{eff}, \omega) = \frac{1 - \sqrt{\epsilon_{eff} - j\sigma_{eff}/\omega\epsilon_0}}{1 + \sqrt{\epsilon_{eff} - j\sigma_{eff}/\omega\epsilon_0}} \quad (2)$$

$$\delta = \frac{1}{N} \sum_{i=1}^N [|\Gamma_m(\omega_i)| - |\Gamma(\epsilon_{eff}, \sigma_{eff}, \omega_i)|]^2 \quad (3)$$

The results of the method of homogenization [5] and the moment method [6] are used for comparison. To match the same frequency characteristic, the optimum values of ϵ_{eff} and σ_{eff} to be used for the plane-boundary dielectric model are 1.000 and 0.005 S/m, respectively. Figures 3 shows the comparison of this model with those available in the literatures. Cancellation between reflections from various parts of the pyramid surface at a few frequency points can be found in the homogenization model and the moment method model. The narrowband cancellation results in the ripple in the reflectivity characteristics in Figure 3. However, the small ripple may not have much effect in the actual applications of the absorber. Hence, the plane-boundary dielectric model may be used in a simulation tool for design of anechoic chamber.

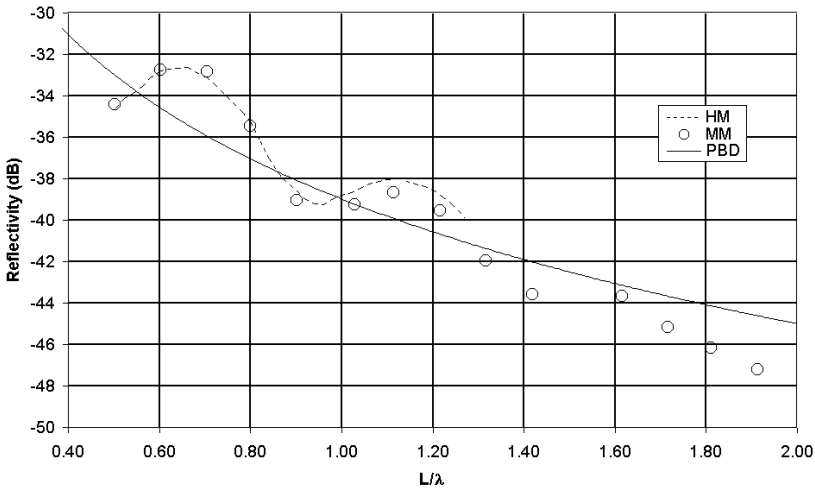


Figure 3. Comparison of reflectivity characteristics between the plane-boundary dielectric model (PBD), homogenization model (HM), and moment method (MM).

For wave incidents at an angle θ_i , the reflection coefficients for parallel and perpendicular polarizations are given by equation (4) and equation (5), respectively.

$$\Gamma_{\parallel} = \frac{\eta_2 \cos \theta_t - \eta_1 \cos \theta_i}{\eta_2 \cos \theta_t + \eta_1 \cos \theta_i} \quad (4)$$

$$\Gamma_{\perp} = \frac{\eta_2 \cos \theta_i - \eta_1 \cos \theta_t}{\eta_2 \cos \theta_i + \eta_1 \cos \theta_t} \quad (5)$$

where η_1 is the wave impedance of free space, η_2 wave impedance of absorber medium, and θ_t angle of refracted wave. The Snell's law of refraction can be written as

$$\sin \theta_t = \frac{1}{\sqrt{\epsilon_r}} \sin \theta_i \quad (6)$$

The reflection coefficients of the plane-boundary lossy dielectric model for parallel and perpendicular polarizations are then given by

$$\Gamma_{\parallel}(\epsilon_{eff}, \sigma_{eff}, \omega) = \frac{\sqrt{(\epsilon_{eff} - j\sigma_{eff}/\omega\epsilon_0) - \sin^2 \theta_i} - (\epsilon_{eff} - j\sigma_{eff}/\omega\epsilon_0) \cdot \cos \theta_i}{\sqrt{(\epsilon_{eff} - j\sigma_{eff}/\omega\epsilon_0) - \sin^2 \theta_i} + (\epsilon_{eff} - j\sigma_{eff}/\omega\epsilon_0) \cdot \cos \theta_i} \quad (7)$$

$$\Gamma_{\perp}(\epsilon_{eff}, \sigma_{eff}, \omega) = \frac{\cos \theta_i - \sqrt{(\epsilon_{eff} - j\sigma_{eff}/\omega\epsilon_0) - \sin^2 \theta_i}}{\cos \theta_i + \sqrt{(\epsilon_{eff} - j\sigma_{eff}/\omega\epsilon_0) - \sin^2 \theta_i}} \quad (8)$$

The degradation of the reflectivity level with respect to angle of incidence can be appropriately evaluated using the plane-boundary dielectric model as shown in Figure 4. For parallel polarization, the lowest reflectivity at the Brewster angle is observed in all three models, although there is a small difference in the Brewster angle. No experimental result is available to evaluate the accuracy of these models.

The plane-boundary dielectric model is particularly suited for use in a ray tracing simulation tool since the absorber-lined surfaces can be easily replaced by a plane with the appropriate ϵ_{eff} and σ_{eff} . The performance of an anechoic chamber depends on the type, size, and array configuration of the absorber elements as well as the geometry of the screened room on which the inner surfaces are covered with the RF absorbers. With suitable anechoic chamber geometry that minimizes reflections to the test region, lower performance RF absorbers can be used to make the anechoic chamber design more economical.

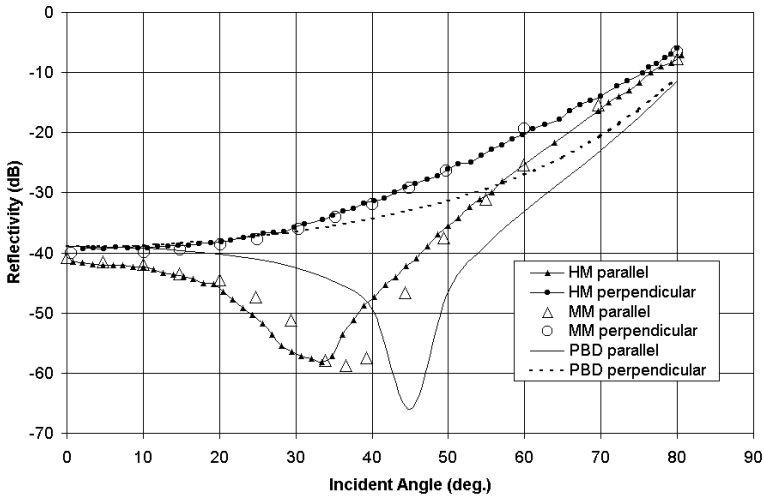


Figure 4. Comparison of oblique scattering characteristics between the plane-boundary dielectric model (PBD), homogenization model (HM), and moment method (MM) for $L/\lambda = 1.016$.

Under the circumstances that the only information available from RF absorber manufacturer's data sheet is the reflectivity magnitude at normal incidence, the planeboundary dielectric model is a good choice. The effectiveness of the RF absorber in actual applications can be reasonably predicted. The use of a complex model may not give a more accurate result due to the various uncertainties involved.

A unique asymmetrical-shaped anechoic chamber has been designed and constructed. The floor plan and cross-sectional views are as shown in Figure 5. With a combination of simple structures, the screened room can easily be constructed and the lining of electromagnetic wave absorbers can properly be controlled.

A 24-inch thick microwave absorber (EMC-24) from Rantec has been used to cover most of the inner surfaces of the anechoic chamber. Based on the reflectivity data from the manufacturer, the plane-boundary dielectric model gives an optimum ϵ_{eff} and σ_{eff} of 1.006 and 0.003 S/m, respectively. Figure 6 shows the comparison of reflectivity characteristic between the model and the manufacturer's data.

The low-frequency (30–1000 MHz) applications of the anechoic chamber is for EMC test. EMC standards specify that a radiated emission test site shall be validated by means of a set of normalized site attenuation (NSA) measurements [7]. The floor shall be a perfectly conducting ground plane. For a 10-meter range, the horizontal distance

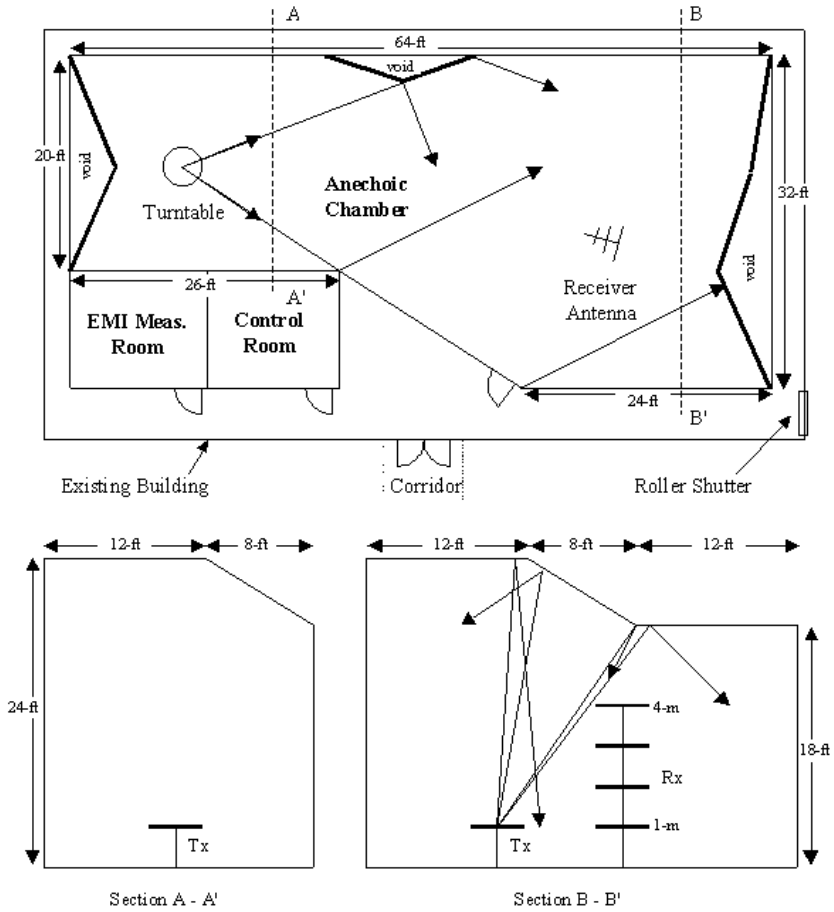


Figure 5. Floor plan and cross-sectional views of the asymmetrical-shaped chamber.

between the transmitter antenna and receiver antenna shall be 10 meters. The receiver antenna scans from 1 to 4 meters heights and the maximum signal voltage measured from this scan is recorded. Site attenuation is defined as the ratio of the voltage input to a matched and balanced lossless radiator to that at the output of a similarly matched balanced lossless receiver antenna. NSA is calculated by dividing the site attenuation with the antenna factors of the transmitter and receiver antennas. A measurement site is considered acceptable for compliance test purposes if the measured NSAs are within 4 dB of the theoretical NSA for an ideal site. For an anechoic chamber, a single-

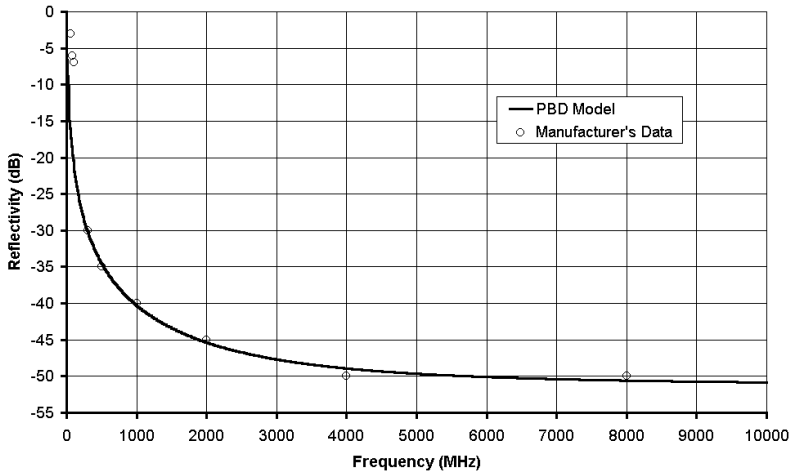


Figure 6. Comparison of reflectivity characteristics between the plane-boundary dielectric (PBD) model and the manufacturer's data.

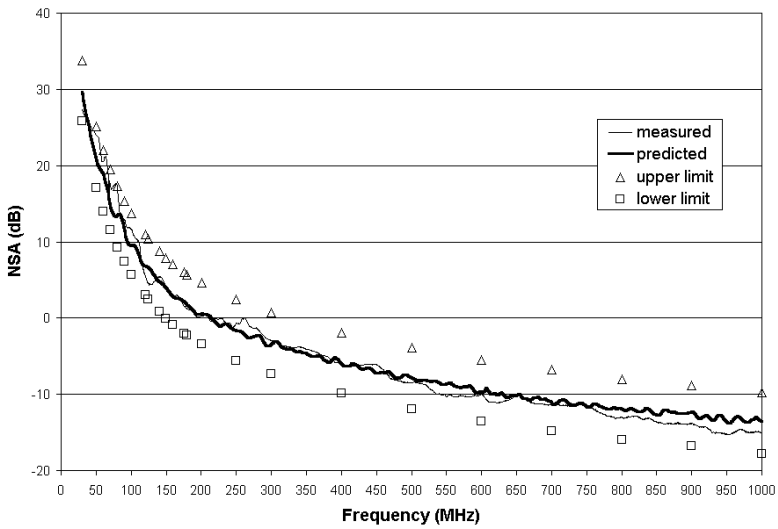


Figure 7. Comparison between measured and predicted NSA (horizontal polarization).

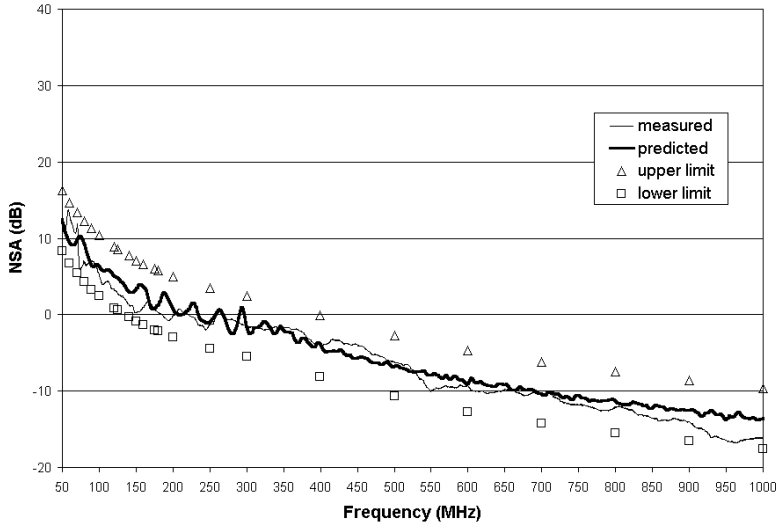


Figure 8. Comparison between measured and predicted NSA (vertical polarization).

point NSA measurement is insufficient to pick up possible reflections from the chamber structure and RF absorbers. The transmitting antenna shall be moved to a few places at the source region and the NSA for each transmitter-receiver setup shall be evaluated. Figure 7 is a sample of the NSA prediction and measurement results for horizontal polarization. The NSA for vertical polarization is shown in Figure 8. These results conform to the limits of ANSI C63.4 standards over the frequency range 30–1000 MHz.

4. CONCLUSIONS

A model has been developed for pyramidal RF absorber with pyramid length shorter than a quarter wavelength and poor reflectivity performance. Since the reflection from the metal backing would be much higher than the reflection and scattering from the pyramid tips, the metal boundary may be modeled as a lossy dielectric with certain effective dielectric constant, ϵ_{eff} , and effective conductivity, σ_{eff} , and the thickness extends to infinity. The appropriate values of ϵ_{eff} and σ_{eff} can be derived based on the reflectivity information given by the manufacturer's data sheet. The plane-boundary dielectric model can be used to evaluate the degradation of reflectivity level with respect to angle of incidence. It can be used in a simulation tool for design of

anechoic chamber.

ACKNOWLEDGMENT

This study is partially funded by the Malaysian Centre for Remote Sensing of the Ministry of Science, Technology and the Environment, Malaysia.

REFERENCES

1. Emerson, W. H., "Electromagnetic wave absorbers and anechoic chambers through the years," *IEEE Transactions on Antennas and Propagation*, 484–490, July 1973.
2. Holloway, C. L., R. R. DeLyser, R. F. German, P. McKenna, and M. Kanda, "Comparison of electromagnetic absorber used in anechoic and semi-anechoic chambers for emission and immunity testing of digital devices," *IEEE Transactions on EMC*, Vol. 39, No. 1, 33–47, February 1997.
3. Pues, H., "Electromagnetic absorber measurement in a large waveguide," *8th International Symposium on EMC*, 253–258, Zurich, 1989.
4. Pues, H., "Electromagnetic absorber measurement in a large coax," *9th International Symposium on EMC*, 541–546, Zurich, 1991.
5. Kuester, E. F. and C. L. Holloway, "Improved low-frequency performance of pyramidal-cone absorbers for application in semi-anechoic chambers," *1989 IEEE International Symposium on EMC*, 394–398, 1989.
6. Janaswamy, R., "Oblique scattering from lossy periodic surfaces with application to anechoic chamber absorbers," *IEEE Transactions on Antennas & Propagation*, Vol. 40, 162–169, 1992.
7. "Methods of measurement of radio-noise emissions from low-voltage electrical and electronic equipment in the range of 9 kHz to 40 GHz," American National Standard Institute, Std. C63.4-1992, July 1992.